Pergamon

Tetrahedron 58 (2002) 7251–7258

TETRAHEDRON

Oligosaccharide binding to a boronic-acid-appended phenanthroline·Cu(I) complex which creates superstructural helicates and catenates

Masashi Yamamoto, Masayuki Takeuchi and Seiji Shinkai*

Department of Chemistry and Biochemistry, Graduate School of Engineering, Kyushu University, Fukuoka 812-8581, Japan

Received 29 May 2002; accepted 1 July 2002

Abstract—Compound **2** bearing two boronic acid moieties at two sides of a 1,10-phenanthroline moiety was synthesized. **2** forms a 1:2 complex with Cu(I) and four boronic acid groups are arranged in the peripheral positions around the central metal chelate. When a saccharide guest links two boronic acid groups in the different ligands, the resultant structure is classified into a helicate, whereas when a saccharide guest links two boronic acid groups in the same ligands, the resultant structure is classified into a catenate. Careful examination of the CD spectra of $\mathbf{2}_2$·Cu(I) complex with saccharides established that (i) the D-glucose complex gives the helicate with P-helicity, (ii) the maltose complex give the helicate with M-helicity, (iii) the maltopentaose and maltohexaose complexes give the catenate with P-helicity, and (iv) maltotriose and maltotetraose cannot provide the stable complex with $\mathbf{2}_2$·Cu(I). The results indicate that $\mathbf{2}_2$·Cu(I) can act as a versatile core to create various superstructures using a boronic acid–saccharide interaction. © 2002 Elsevier Science Ltd. All rights reserved.

1. Introduction

Topological chemistry related to catenates and rotaxanes is, presently, the hottest research area in supramolecular chemistry.[1–6] They not only enable us to create novel stereochemical architectures but also serve as unique scaffolds for electron or energy transfer, catalytic reactions, units of molecular assemblies, etc.[1–6] It is also demonstrated that reflecting their inherent characteristies that each molecular unit is linked by noncovalent bonds, these molecular systems frequently show 'dynamic' properties which are affected by their milieu.[7–9] Here, it occurred to us that if these superstructures could be produced under some equilibrium, it would mean that these potential scaffolds are created in response to 'chemical signals'. We previously designed compounds **1a** and **1b** which have a 1,10-phenanthroline moiety and a boronic acid moiety.[10] These compounds formed a helical structure in the presence of Cu(I), and when saccharides were added, the Cu(I) complexes gave the CD-active species arising from an equilibrium shift in the P versus M helicity of the helical complexes.[10] The results show that the terminal boronic acid group is useful to create the chiral helical structure and the total helicity is governed by the chirality of the boronic acid-bound saccharide (Scheme 1).

When we were seeking for the stable structures of these ligand–Cu(I)–saccharide ternary complexes by a computational method, we noticed an interesting possibility that compound **2** bearing two boronic acid moieties at two sides of a 1,10-phenanthroline moiety could result in either helicates with short mono- and disaccharides or catenates with long oligosaccharides (Scheme 2: helicate is a D-glucose (M1) complex whereas catenate is a maltopentaose complex: both structures are energy-minimized by a computational method using Discover 3/Insight II 98.0). In the helicates saccharides are linked with boronic acid groups in the different ligands whereas in the catenates they are linked with boronic acid groups in the same ligands. With these fascinating working hypotheses in mind, we tried to find evidence for the selective formation of helicates and catenates from the same molecular unit.

2. Results and discussion

2.1. Spectral characterizations of the Cu(I) complex

Spectral examinations were carried out in MeOH/MeCN=100:1 (v/v) at 25°C to avoid aggregation of the complex (in fact, it occurred, e.g. in water[10]). Fig. 1 shows the absorption spectral change induced by the Cu(I) addition (added as $[Cu(MeCN)_4]ClO_4$). The λ_{max} at 305.5 nm decreased while that at 439.5 nm increased with tight isosbestic points at 256.5 and 365.0 nm. The plots of the absorbances at 330.5, 341.0, and 439.5 nm (where large

Keywords: superstructural helicates and catenates; helicity; oligosaccharide binding.

* Corresponding author. Tel.: +81-92-642-3583; fax: +81-92-642-3611; e-mail: seijitcm@mbox.nc.kyushu-u.ac.jp

0040–4020/02/$ - see front matter © 2002 Elsevier Science Ltd. All rights reserved.
PII: S0040-4020(02)00786-X

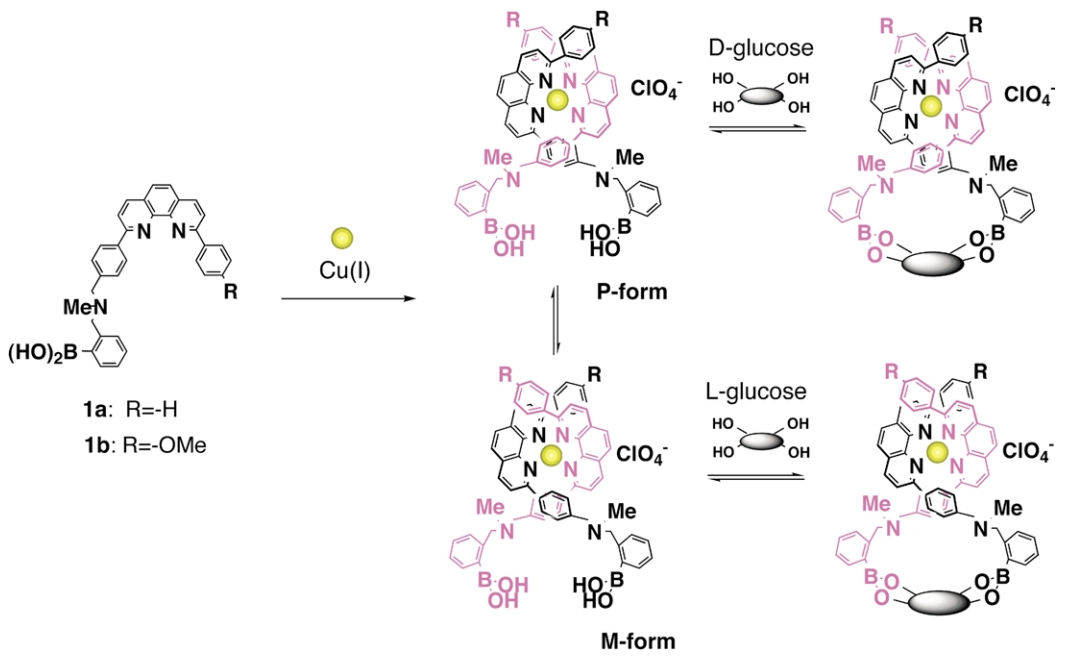

Scheme 1.

spectral changes were observed) against [Cu(I)]/[**2**] (Fig. 2) afforded a clear break-point at 0.5, indicating that the complex consists of one Cu(I) and two **2** ligands (as illustrated in Scheme 2).

This stoichiometry was also confirmed by ESI-mass spectroscopy (ESI-MS). When a solution containing **2** (0.200 mmol dm^{-3}) and $[Cu(MeCN)_4]ClO_4$ (0.100 mmol dm^{-3}) was subjected, the parent peak $[\mathbf{2}_2{\cdot}Cu(I)]^+$ was observed at m/z=1435.3. In addition, the eight larger peaks with $\Delta\ m/z=n$ ($MeOH-H_2O$) (where n=1–8) were observed, indicating that the $B(OH)_2$ groups were partly converted to the $B(OMe)_2$ in the present MeCN/MeOH=100:1 (v/v) solvent. The $\mathbf{2}_2{\cdot}Cu(I)$ structure was also supported by the ^1H NMR spectrum measured in MeOD-d_4/MeCN-d_3=100:1 (v/v) (see Section 4).

2.2. Saccharide-induced CD spectral changes

To obtain insights into the superstructure of $\mathbf{2}_2{\cdot}Cu(I)$–saccharide complexes we measured CD spectra in the presence of six different saccharides (Fig. 3). It is seen from Fig. 3 that saccharide addition yields the CD-active species and both the CD activity and the CD sign are dependent upon the type of used saccharides.

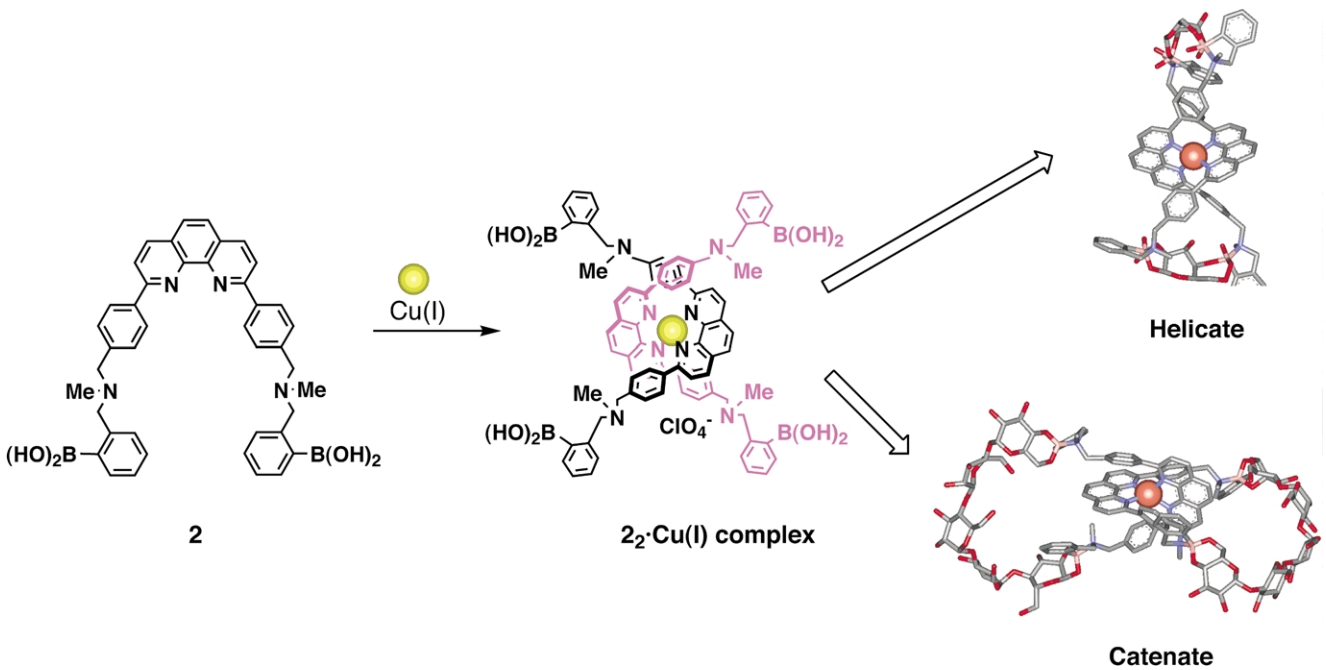

Scheme 2.

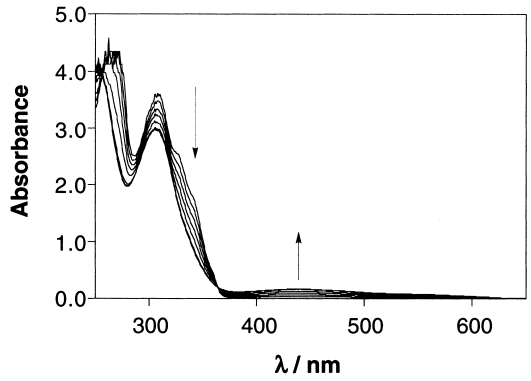

Figure 1. Absorption spectral change of **2** (0.100 mmol dm^3) with increasing Cu(I) concentration.

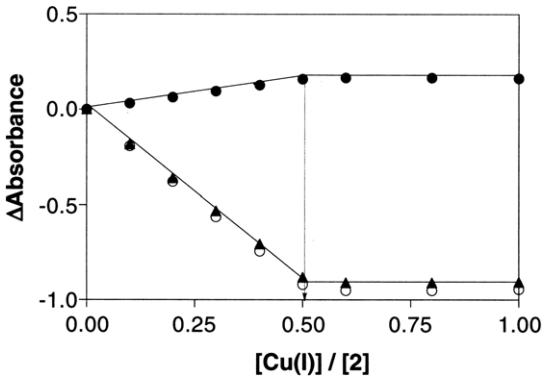

Figure 2. Plots of absorbance versus [Cu(I)]/[**2**]: ○, 330.5 nm; ▲, 341.0 nm; ●, 439.5 nm.

Fig. 4 shows plots of CD intensities versus saccharide concentrations. It is seen from Fig. 4 that the plots consist of simple saturation curves. The finding, together with the presence of tight isosbestic points in the CD spectra of Fig. 3, supports the view that one (or more than one) **2**$_2$·Cu(I)·saccharide ternary complex is monotonously formed with increasing saccharide concentrations and a sudden change from one species to other species (e.g. from helicate to catenate) does not take place with the same saccharide.

Before the discussion on the helicity, however, one must

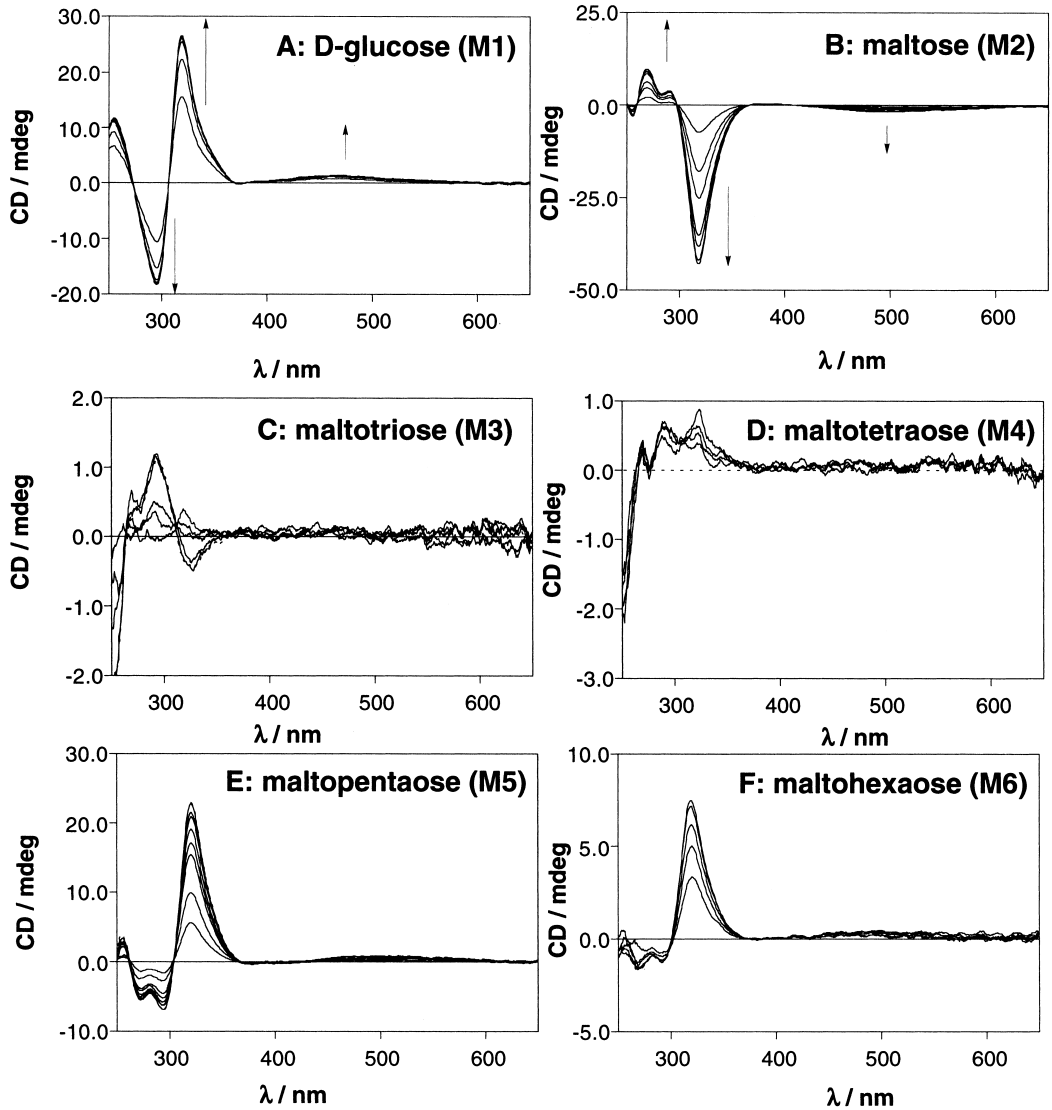

Figure 3. CD spectra of **2**$_2$·Cu(I) complex (0.100 mmol dm^3) in the presence of saccharides (0–25.0 mmol dm^3: the highest concentration for maltohexaose (M6) is 11.7 mmol dm^3 because of the solubility limitation.

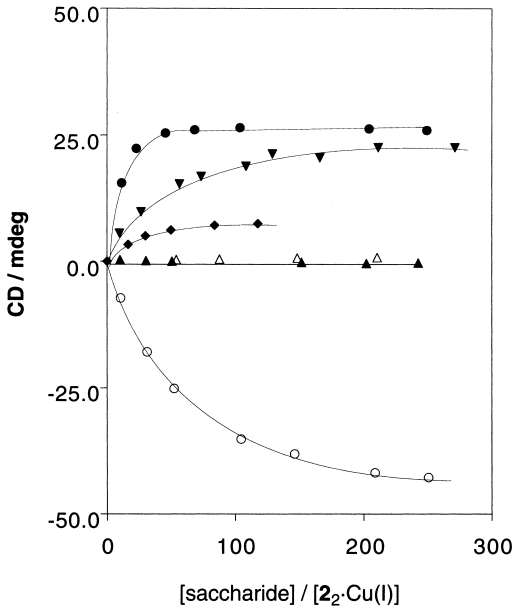

Figure 4. Plots of CD intensities versus saccharide concentrations: [$\mathbf{2}_2$·Cu(I)]=0.100 mmol dm^3; •, D-glucose (at 319.0 nm); ○, maltose (at 318.5 nm); ▲, maltotriose (at 320.5 nm); △, maltotetraose (at 320.5 nm); ▼, maltopentaose (at 320.5 nm); ◆, maltohexaose (at 320.5 nm).

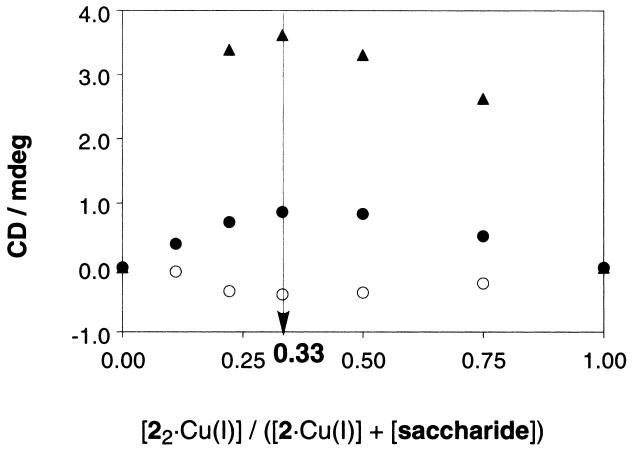

Figure 5. Job plots: the concentration of $\mathbf{2}_2$·Cu(I)+saccharide was maintained constant (0.200 mmol dm^3). The CD intensities used here were 319.0 nm for M1 (▲) and 321.0 nm for M2 (○), and M5 (•) where the CD changes are largest.

confirm whether two saccharide molecules are really bound to $\mathbf{2}_2$·Cu(I) complex, as illustrated in Scheme 2. The Job plots for D-glucose, maltose, and maltohexaose (Fig. 5) always show a clear break point at 0.33, indicating complex can binds two saccharides. Now, we can discuss the superstructures of $\mathbf{2}_2$·Cu(I)·(saccharides)$_2$ ternary complexes on the basis of the CD sign. We previously observed for $\mathbf{1a}_2$·Cu(I)·glucose ternary complexes that D-glucose gives the positive CD sign at the MLCT region (400–600 nm) and the positive exciton-coupling band at the $\pi-\pi^*$ region (at around 310 nm) whereas L-glucose gives the symmetrical spectral pattern to that of D-glucose.[10] The past CD studies on chiral bipyridine-based helicate–Cu(I) complexes have established that the positive CD sign at the MLCT region is generated from the P-isomer whereas the negative CD sign is generated from the M-isomer.[11–13] This means that D-glucose twists the $\mathbf{1a}_2$·Cu(I) complex into the P chirality motif (clockwise direction around the central axis connecting Cu(I) with glucose) whereas L-glucose twists it into the M chirality motif. Examination of Figs. 3 and 4 reveals that in $\mathbf{2}_2$·Cu(I), the D-glucose complex has the P chirality motif as in the case of $\mathbf{1a}_2$·Cu(I)·D-glucose whereas the maltose complex has the M chirality motif as in the case of $\mathbf{1a}_2$·Cu(I)·L-glucose. It is known that in the boronic acid–oligosaccharide complexation, diboronic-acid-based receptors tend to bind the 1,2-diol group in the right pyranose ring and the 4,6-diol group in the left pyranose ring.[14] One may regard, therefore, that a change from D-glucose (M1) to maltose (M2) increases the distance between the two boronic acid moieties and as a result P-helicity is converted to M-helicity. In the presence of maltotriose (M3) and maltotetraose (M4) the CD intensity was scarcely observable. In the presence of maltopentaose (M5) and maltohexaose (M6) the CD intensity became strong again and the helicity was judged to be P from the CD sign. These spectral results indicate that the M1 and M2 complexes with $\mathbf{2}_2$·Cu(I) are similar to those with $\mathbf{1a}_2$·Cu(I); in contrast, the M5 and M6 complexes with $\mathbf{2}_2$·Cu(I) are quite different from those with $\mathbf{1a}_2$·Cu(I).

2.3. Helicate versus catenate formation from $\mathbf{2}_2$·Cu(I) complex

From CPK molecular modelling studies and their computational optimization studies, we noticed that in $\mathbf{2}_2$·Cu(I) complex the distance between the two boronic acid moieties in the different ligands is a little shorter than that in the same ligand. Furthermore, 5,6-hydrogens of the 1,10-phenanthroline moiety partially intrude into the space between the two boronic acid moieties in the same ligands. As a result, the oligosaccharide bound to these two boronic acid moieties must be bent like an arc, keeping it away from this steric crowding. These preconsiderations suggest that short M1 and M2 tend to result in helicates whereas long M5 and M6 tend to result in catenates. It seems to be very difficult, however, to assign the structure of $\mathbf{2}_2$·Cu(I)·saccharide ternary complexes either to helicates or to catenates by spectroscopic methods, because they are all formed under

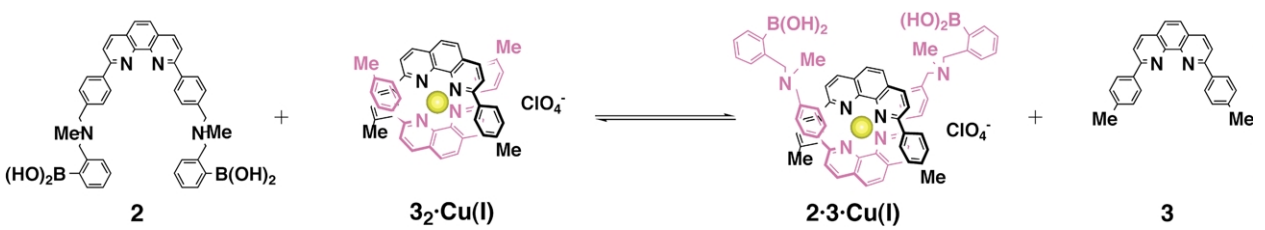

Scheme 3.

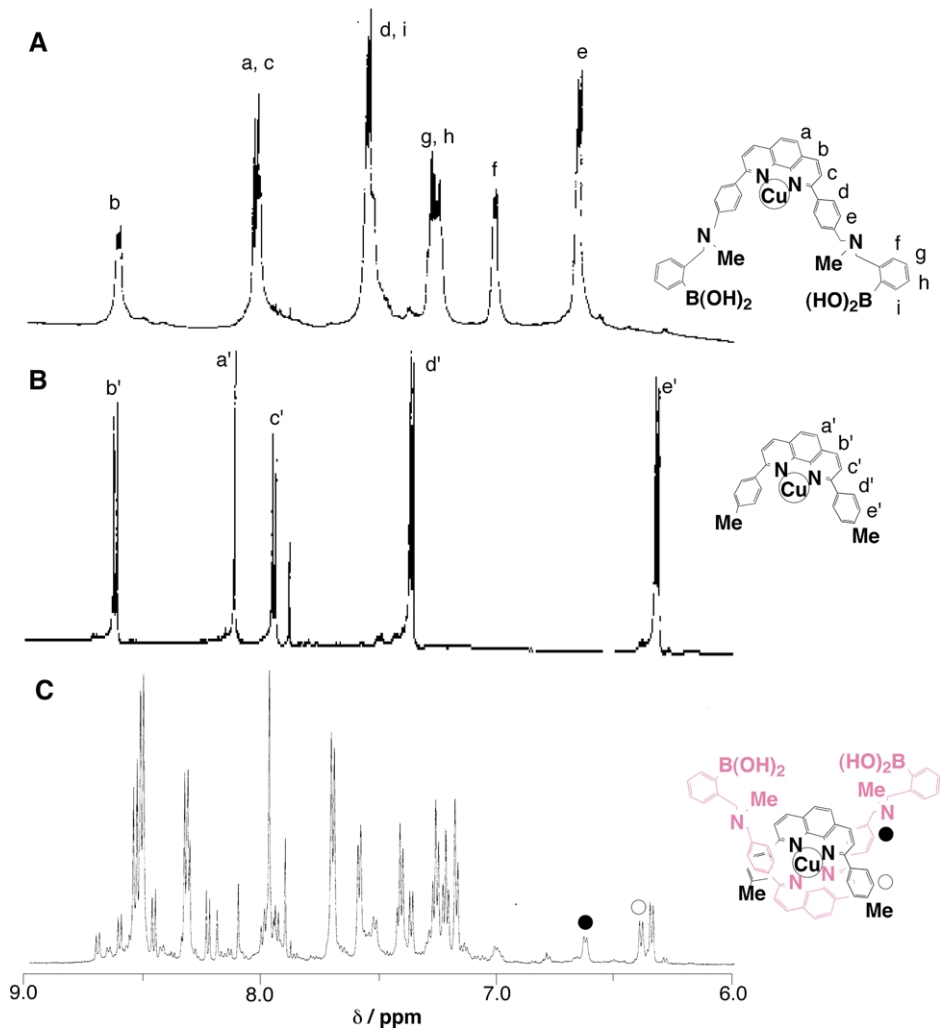

Figure 6. Partial ^{1}H NMR spectra of $\mathbf{2}_2$·Cu(I), $\mathbf{3}_2$·Cu(I), and **2**·**3**·Cu(I) complexes in MeOH-d_4/MeCN-d_3=100:1 (v/v) at 25°C.

equilibria and the molecular symmetry is similar to each other.

Here, we adopted a realistic method to compare the CD spectral pattern of $\mathbf{2}_2$·Cu(I)·saccharide ternary complexes with those of 'authentic' helicate and catenate samples. The $\mathbf{1b}_2$·Cu(I)·saccharide ternary complexes in which the saccharide can only link two boronic acid moieties in the different ligands are useful as the authentic samples for helicates. To prepare the authentic samples for catenates we mixed **2** with a 2,9-di(4-tolyl)-1,10-phenanthroline (**3**)/Cu(I)=2:1 complex ($\mathbf{3}_2$·Cu(I)). As long as $\mathbf{3}_2$·Cu(I) exists over **2**, the major species in this solution are unreacted $\mathbf{3}_2$·Cu(I) and exchanged hetero-complex **2**·**3**·Cu(I) (Scheme 3). Since $\mathbf{3}_2$·Cu(I) is CD-silent, one can obtain the CD spectral pattern arising from a catenate mimic complex, **2**·**3**·Cu(I) in which the saccharide can only link two boronic acid moieties in the same ligand.

The formation of **2**·**3**·Cu(I) from **2** and $\mathbf{3}_2$·Cu(I) in MeOH/MeCN=100:1 (v/v) at 25°C was monitored by ESI-MS, maintaining the concentration of $\mathbf{3}_2$·Cu(I) constant (0.100 mmol dm^{-3}) while varying the concentration of **2** (0.100–0.400 mmol dm^{-3}). The peaks assignable to **2**·**3**·Cu(I) (m/z=783.3) and **2**·**3**·Cu(I)·n(MeOH–H_2O) (Where n=1–4) were increased with the increase in added **2** concentration. However, the peaks assignable to $\mathbf{2}_2$·Cu(I) and its MeOH adducts were not detected even at [added **2**]/[$\mathbf{3}_2$·Cu(I)]=4.0. Presumably, the association constant of **2** with Cu(I) may be smaller than that of **3** with Cu(I). Next, we tried to detect the formation of **2**·**3**·Cu(I) complex by ^{1}H NMR spectroscopy at [$\mathbf{3}_2$·Cu(I)]/[added **2**]=4.0 in MeOD-d_4/MeCN-d_3=100:1 (v/v) at 25°C (Fig. 6). As expected, all peaks for the Cu(I)-coordinated species were assigned to $\mathbf{3}_2$·Cu(I) and **2**·**3**·Cu(I). From the intergral intensity of the 6.39 (3,5-protons of 4-tolyl moiety in **3**) (or 6.64: 3,5-protons of 4-benzyl moiety in **2**) ppm peak for **2**·**3**·Cu(I) versus the 6.35 ppm peak for $\mathbf{3}_2$·Cu(I) (3,5-protons of 4-tolyl moiety in **3**), the ratio of **2**·**3**·Cu(I): $\mathbf{3}_2$·Cu(I) was estimated to be 0.83:1.0. This mixture was subjected to the CD measurements in the presence of saccharides.

Examination of their CD spectra (Fig. 7) reveals that the spectral pattern of the $\mathbf{2}_2$·Cu(I)+D-glucose having a positive band at the MLCD region and a positive exciton-coupling band at the π–π^* region is basically consistent with that of the $\mathbf{1b}_2$·Cu(I)+D-glucose helicate complex but different from that of the **2**·**3**·Cu(I)+D-glucose catenate mimic complex (Fig. 7(A)). The results indicate that $\mathbf{2}_2$·Cu(I) results in a helicate in which one D-glucose molecule link

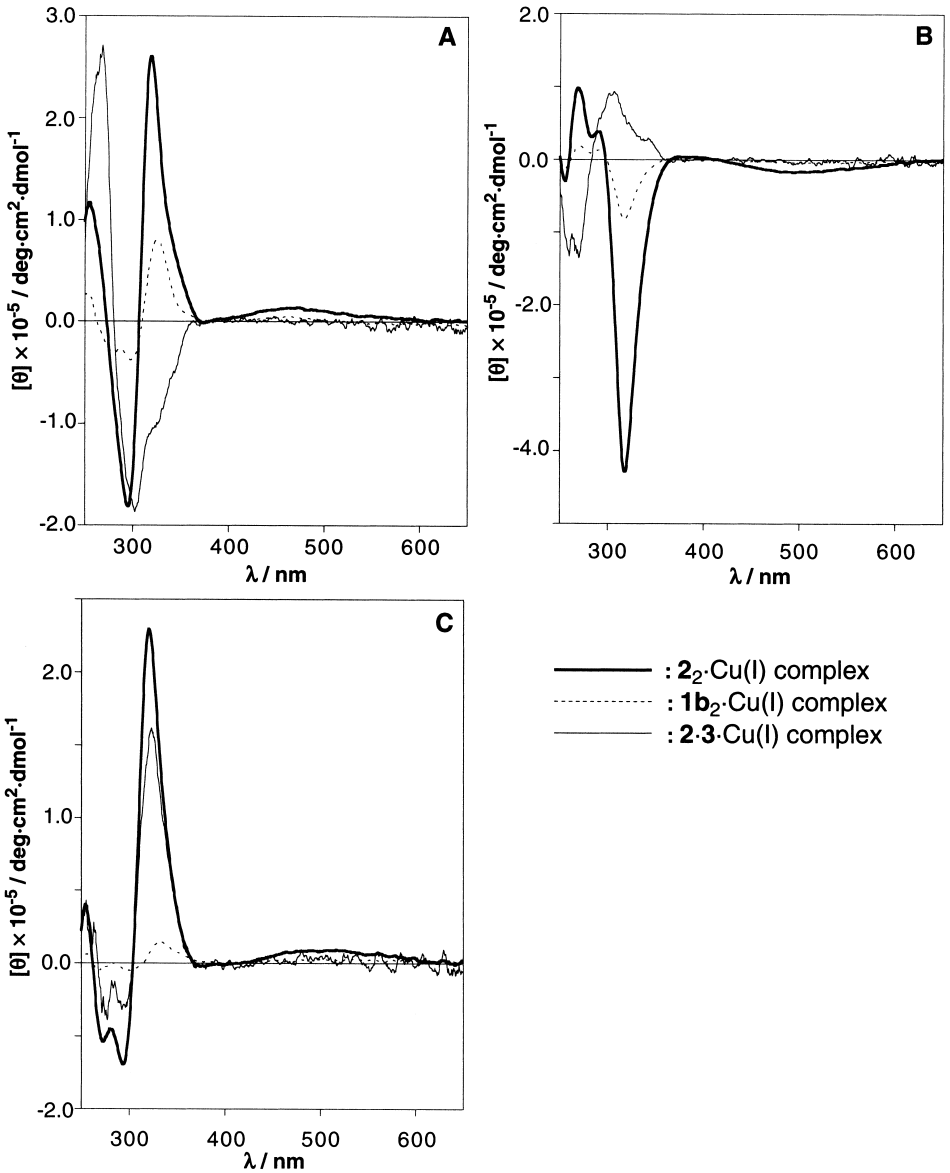

Figure 7. CD spectra of $\mathbf{2}_2$·Cu(I), $\mathbf{1b}_2$·Cu(I) affording only helicates, and **2**·**3**·Cu(I) affording only catenate mimics in the presence of (A) M1, (B) M2, and (C) M5: [$\mathbf{1b}_2$·Cu(I)]=0.200 mmol dm^3, [$\mathbf{2}_2$·Cu(I)]=0.200 mmol dm^3, **2**·**3**·Cu(I) obtained from [**2**]=0.400 mmol dm^3 and [$\mathbf{3}_2$·Cu(I)]=0.100 mmol dm^3, [saccharide]=25.0 mmol dm^3.

Table 1. CD spectral parameters

	$\mathbf{2}_2$·Cu(I) complex		$\mathbf{1b}_2$·Cu(I) complex		**2**·**3**·Cu(I) complex[a]	
	$\pi-\pi^*$ absorption band $[\theta]_{max\ or\ min}\times10^{-5}$, deg cm^2 dmol^{-1} ($\lambda_{max\ or\ min}$, nm)					
	First	Second	First	Second	First	Second
D-Glucose (M1)	2.60 (319.0)	−1.81 (295.5)	0.81 (325.0)	−0.38 (297.5)	−1.87 (302.5)	2.71 (268.0)
Maltose (M3)	−4.29 (322.0)	0.39 (290.5)	−0.85 (317.0)	0.13 (289.5)	0.94 (306.5)	−1.35 (296.5)
Maltotriose (M3)	−0.05 (327.5)	0.11 (293.0)	0.25 (317.0)	−0.09 (287.5)	0.60 (298.5)	−0.65 (271.5)
Maltotetraose (M4)	0.07 (288.5)	–	−0.07 (318.5)	0.05 (292.5)	0.62 (305.0)	−0.75 (262.5)
Maltopentaose (M5)	2.29 (320.5)	−0.69 (294.0)	0.15 (332.0)	0.05 (298.5)	1.62 (323.0)	−0.32 (292.0)
Maltohexaose (M6)	−0.75 (319.0)	−0.12 (332.0)	0.05 (332.0)	0.02 (298.5)	0.79 (321.0)	0.50 (270.0)

[a] $[\theta]_{max\ or\ min}$ values in this column are 'observed' values for the mixture of **3** and **2**·**3**·Cu(I)·saccharide.

two boronic acid moieties in the different ligands. Fig. 7(B) shows that $\mathbf{2}_2$·Cu(I) gives the CD spectrum similar to that of $\mathbf{1b}_2$·Cu(I), indicating that again, the helicate is yielded with maltose. With maltopentaose, on the other hand, the CD spectrum for $\mathbf{2}_2$·Cu(I) is similar to that for **2**·**3**·Cu(I), indicating that this oligosaccharide binds two boronic acid moieties in the same ligands to form a catenate molecule. We carried out this kind of comparative experiments for six saccharides from D-glucose (M1) to maltohexaose (M6). The CD paramers are summarized in Table 1. It is seen from this table that (i) M1 and M2 tend to from helicates with $\mathbf{2}_2$·Cu(I), (ii) M5 and M6 tend to form catenates, and (iii) M3 and M4 cannot from either stable helicates or catenate.

3. Conclusions

Helicates and catenates are representative supramolecular families among superstructural architectures. The present study has demonstrated that these fascinating architectures can be derived from a single molecular unit utilizing a boronic acid–saccharide interaction: that is, when two pairs of bis(boronic acid) groups are spatially arranged, the saccharide links either interligand or intraligand bis(boronic acid) groups, depending on the length of the used saccharide. These cross-linking modes result in either the helicate or the catenate. The finding implies that the multi-point interaction between bis(boronic acid) groups and saccharides can become a new idea source for molecular design of superstructures, including chirality, OH-based hydrogen-bonding sites, physiological activities, etc. inherent to saccharides. Furthermore, we believe that when some catalytic sites such as porphyrins,[14,15] Ru(II)(bpy)$_3$,[16] Co(II)salen,[17] etc. are introduced into these superstructures as their boronic acid derivatives, they should show novel catalytic or photochemical functions. Further studies are currently continued in our laboratory.

4. Experimental

4.1. Materials

Syntheses of compounds **1a** and **1b** were reported previously.[10] 2,9-Di(4-tolyl)-1,10-phenanthroline (**3**) was prepared according to the method of Goodman et al.[18] and identified by IR and ^{1}H NMR spectral evidence and elemental analysis.

4.2. Synthesis

Compound **2** was synthesized from **3** according to the method reported previously.[10] Here, we show only its analytical data.

4.2.1. Compound 2. Light yellow powder; mp>300°C; IR (KBr, cm^{-1})=3414 (νO–H), 1344 (νB–O); ^{1}H NMR (600 MHz, $CDCl_3$, TMS, 25°C), δ/ppm=2.30 (s, 3H, –NCH_3), 3.64 (s, 2H, –CH_2), 3.72 (s, 2H, –CH_2), 7.23 (d, J=6.8 Hz, 1H, Ar-H), 7.37 (t, J=6.5 Hz, 2H, Ar-H), 7.56 (d, J=7.8 Hz, 2H, Ar-H), 7.77 (d×2, J=8.9 Hz, 2H, Ar$_{phen}$-H), 7.78 (s, 1H, Ar$_{phen}$-H), 8.07 (d, J=6.6 Hz, 1H, Ar-H), 8.12 (d, J=8.3 Hz, 1H, Ar$_{phen}$-H), 8.30 (d, J=8.4 Hz, 1H, Ar$_{phen}$-H), 8.30 (d, J=8.4 Hz, 1H, Ar$_{phen}$-H), 8.47 (d, J=7.7 Hz, 2H, Ar-H); calcd for $C_{42}H_{40}N_4O_4B_2$: C, 73.49; H, 5.87; N, 8.16%; found: C, 73.63; H, 5.67; N, 7.84%.

4.3. Miscellaneous

^{1}H NMR, absorption spectra, ESI-MS spectra and CD spectra were measured with Bruker DMX 600, Shimadzu UV-2500, Perseptive Mariner and JASCO J-720 WI, respectively.

Acknowledgments

This work was supported by a Grant-in-Aid for COE Research 'Design and Control of Advanced Molecular Assembly Systems' from the Ministry of Education, Science and Culture, Japan (#08CE2005).

References

1. (a) Asakawa, M.; Ashton, P. R.; Balzani, V.; Credi, A.; Hamers, C.; Mattersteig, G.; Montalti, M.; Shipway, N.; Spencer, N.; Stoddart, J. F.; Tolley, M. A.; Venturi, A.; White, A. J. P.; Williams, D. J. *Angew. Chem., Int. Ed. Engl.* **1998**, *37*, 333. (b) Balzani, V.; Credi, A.; Raymo, F. M.; Stoddart, J. F. *Angew. Chem., Int. Ed. Engl.* **2000**, *39*, 3348. (c) Pease, A. R.; Jeppesen, J. O.; Stoddart, J. F.; Luo, Y.; Collier, C. P.; Heath, J. R. *Acc. Chem. Res.* **2001**, *34*, 433. (d) Stoddart, J. F.; Tseng, H.-R. *Proc. Natl Acad. Sci.* **2002**, *99*, 4797.
2. (a) Sauvage, J.-P. *Acc. Chem. Res.* **1998**, *31*, 405. (b) Armaroi, N.; Balzani, V.; Collin, J.-P.; Gavina, P.; Sauvage, J.-P.; Ventura, B. *J. Am. Chem. Soc.* **1999**, *121*, 4397. (c) Consuelo Jimenez, M.; Dietrich-Buchecker, C. O.; Sauvage, J.-P. *Angew. Chem., Int. Ed. Engl.* **2000**, *39*, 3284. (d) Collin, J.-P.; Dietrich-Buchecker, C.; Gavina, P.; Jimenez-Molero, M. C.; Sauvage, J.-P. *Acc. Chem. Res.* **2001**, *34*, 477.
3. (a) Schalley, C. A.; Beizai, K.; Vögtle, F. *Acc. Chem. Res.* **2001**, *34*, 465. (b) Seel, C.; Parham, A. H.; Safarowsky, O.; Huebner, G. M.; Vögtle, F. *J. Org. Chem.* **1999**, *64*, 7236. (c) Yamamoto, C.; Okamoto, Y.; Schmidt, T.; Jaeger, R.; Vögtle, F. *J. Am. Chem. Soc.* **1997**, *119*, 10547. (d) Vögtle, F.; Duennwald, T.; Schmidt, T. *Acc. Chem. Res.* **1996**, *29*, 451.
4. (a) Bermudez, V.; Carron, N.; Gase, T.; Gatti, F. G.; Kajzar, F.; Leigh, D. A.; Zerbetto, F.; Zhang, S. *Nature* **2000**, *406*, 608. (b) Wurpel, G. W.; Brouwer, A. M.; van Stokkum, I. H.; Farran, A.; Leigh, D. A. *J. Am. Chem. Soc.* **2001**, *123*, 11327. (c) Gatti, F. G.; Leigh, D. A.; Nepogodiev, S. A.; Slawin, A. M.; Teat, S. J.; Wong, J. K. *J. Am. Chem. Soc.* **2001**, *123*, 5983. (d) Brouwer, A. M.; Frochot, C.; Gatti, F. G.; Leigh, D. A.; Mottier, L.; Paolucci, F.; Roffia, S.; Wurpel, G. W. *Science* **2001**, *291*, 2124.
5. (a) Harada, A. *Acc. Chem. Res.* **2001**, *34*, 456. (b) Shigekawa, H.; Miyake, K.; Sumaoka, J.; Harada, A.; Komiyama, M. *J. Am. Chem. Soc.* **2000**, *122*, 5411. (c) Harada, A.; Kamachi, M. *Macromolecules* **1990**, *23*, 2821. (d) Harada, A.; Li, J.; Kamachi, M. *Nature* **1992**, *356*, 325.
6. (a) Hori, A.; Kumazawa, K.; Kusukawa, T.; Chand, D. K.; Fujita, M.; Sakamoto, S.; Yamaguchi, K. *Chem. Eur. J.* **2001**, *7*, 4142. (b) Dietrich-Buchecker, C.; Sauvage, J.-P.; Geum, N.; Hori, A.; Fujita, M.; Sakamoto, S.; Yamaguchi, K. *Chem.*

Commun. **2001**, 1182. (c) Fujita, M.; Fujita, N.; Ogura, K.; Yamaguchi, K. *Nature* **1999**, *400*, 52. (d) Fujita, M. *Acc. Chem. Res.* **1999**, *32*, 53. (e) Fujita, M.; Aoyagi, M.; Ibukuro, F.; Ogura, K.; Yamaguchi, K. *J. Am. Chem. Soc.* **1998**, *120*, 611. (f) Watanabe, N.; Kihara, N.; Takata, T. *Org. Lett.* **2001**, *3*, 3519. (g) Watanabe, N.; Furusho, Y.; Kihara, N.; Takata, T.; Kinbara, K.; Saigo, K. *Bull. Chem. Soc. Jpn* **2001**, *74*, 149. (h) Furusho, Y.; Shoji, J.; Watanabe, N.; Kihara, N.; Adachi, T.; Takata, T. *Bull. Chem. Soc. Jpn* **2001**, *74*, 139.

7. (a) Ballardini, R.; Balzani, V.; Credi, A.; Gandolfi, M. T.; Venturi, M. *Acc. Chem. Res.* **2001**, *34*, 445. (b) Balzani, V.; Credi, A.; Venturi, M. *Proc. Natl Acad. Sci.* **2002**, *99*, 4814.
8. (a) Ashton, P. R.; Ballardini, R.; Balzani, V.; Baxter, I.; Credi, A.; Fyfe, M. C. T.; Gandolfi, M. T.; Gomez-Lopez, M.; Martinez-Diaz, M.-V.; Piersanti, A.; Spencer, N.; Stoddart, J. F.; Venturi, M.; White, A. J. P.; Williams, D. J. *J. Am. Chem. Soc.* **1998**, *120*, 11932. (b) Collier, C. P.; Mattersteig, G.; Wong, E. W.; Luo, Y.; Beverly, K.; Sampaio, J.; Raymo, F. M.; Stoddart, J. F.; Heath, J. R. *Science* **2000**, *289*, 1172.
9. Murakami, H.; Kawabuchi, A.; Kotoo, K.; Kunitake, M.; Nakashima, N. *J. Am. Chem. Soc.* **1997**, *119*, 7605.
10. (a) Yamamoto, M.; Takeuchi, M.; Shinkai, S. *Tetrahedron Lett.* **1998**, *39*, 1189. (b) Yamamoto, M.; Takeuchi, M.; Shinkai, S.; Tani, F.; Naruta, Y. *J. Chem. Soc., Perkin Trans. 2* **2000**, 9.
11. Zarges, W.; Hall, J.; Lehn, J.-M. *Helv. Chim. Acta* **1991**, *74*, 1843.
12. (a) Constable, E. C.; Kulke, T.; Neuburger, M.; Zehnder, M. *Chem. Commun.* **1997**, 489. (b) Baum, G.; Constable, E. C.; Fenske, D.; Housecroft, C. E.; Kulke, T. *Chem. Commun.* **1998**, 2659.
13. Woods, C. R.; Benaglia, M.; Cozzi, F.; Siegel, J. S. *Angew. Chem., Int. Ed. Engl.* **1996**, *35*, 1830.
14. (a) Sugasaki, A.; Ikeda, M.; Takeuchi, M.; Shinkai, S. *Angew. Chem., Int. Ed. Engl.* **2000**, *39*, 3839. (b) Ikeda, M.; Shinkai, S.; Osuka, A. *Chem. Commun.* **2000**, 1047.
15. (a) Takeuchi, M.; Imada, T.; Shinkai, S. *J. Am. Chem. Soc.* **1996**, *118*, 10658. (b) Takeuchi, M.; Chin, Y.; Imada, T.; Shinkai, S. *Chem. Commun.* **1996**, 1867. (c) Takeuchi, M.; Kijima, H.; Hamachi, I.; Shinkai, S. *Bull. Chem. Soc. Jpn* **1997**, *70*, 699. (d) Sugasaki, A.; Ikeda, M.; Takeuchi, M.; Koumoto, K.; Shinkai, S. *Tetrahedron* **2000**, *56*, 4717. (e) Sugasaki, A.; Sugiyasu, K.; Ikeda, M.; Takeuchi, M.; Shinkai, S. *J. Am. Chem. Soc.* **2001**, *123*, 10239.
16. (a) Mizuno, T.; Takeuchi, M.; Hamachi, I.; Nakashima, K.; Shinkai, S. *Chem. Commun.* **1997**, 1793. (b) Mizuno, T.; Takeuchi, M.; Hamachi, I.; Nakashima, K.; Shinkai, S. *J. Chem. Soc., Perkin Trans. 2* **1998**, 2281.
17. (a) Mizuno, T.; Takeuchi, M.; Shinkai, S. *Tetrahedron* **1999**, *55*, 9455. (b) Mizuno, T.; Yamamoto, M.; Takeuchi, M.; Shinkai, S. *Tetrahedron* **2000**, 6193.
18. Goodman, M. S.; Hamilton, A. D.; Weiss, J. *J. Am. Chem. Soc.* **1995**, *117*, 8447.